J Supercond Nov Magn (2014) 27:2555–2562
DOI 10.1007/s10948-014-2624-y

ORIGINAL PAPER

A Comparison of the Effects of Sm and Pb Doping in $Bi_4O_4S_3$ Superconductor

Xiong Yao · Jifeng Shao · Zhongheng Liu · Lei Zhang · Shun Tan · Changjin Zhang · Yuheng Zhang

Received: 16 June 2014 / Accepted: 2 July 2014 / Published online: 20 July 2014

Abstract The effects of isovalent Sm doping and bivalent Pb doping at the Bi site on the superconductivity of $Bi_4O_4S_3$ superconductor are studied and compared. It is found that the bivalent Pb doping results in much faster decrease of superconducting transition temperature and upper critical field, compared with the isovalent Sm doping. Hall effect measurements suggest that bivalent Pb doping gives rise to rapid decrease in electron-like charge carrier concentration. Our results indicate that the bivalent Pb ions not only act as the impurity scatterers but also introduce hole-type charge carriers, which is harmful to the superconductivity in $Bi_4O_4S_3$ system.

Keywords Doping · Magnetization and resistivity · Hall effect

1 Introduction

The discovery of superconductivity in Fe-based compounds has sparked renewed interest in the exploration of new superconductors in materials with layered crystal structure [1, 2]. The recently discovered BiS_2-based superconductors have attracted enormous attention because they enrich the physics and chemistry of layered superconductors [3, 10]. After the discovery of $Bi_4O_4S_3$, a series of BiS_2-based superconductors have been synthesized, such as $REO_{1-x}F_xBiS_2$ (RE = La, Ce, Nd, Pr) [5, 8] and $Sr_{1-x}La_xFBiS_2$ [9, 10]. The superconducting transition temperature of these compounds can be as high as 10 K. Structurally, the $Bi_4O_4S_3$ superconductor is composed of a stacking of alternative $Bi_4O_4(SO_4)_{1-x}$ blocking layers and BiS_2 superconducting layers [3]. First-principle band structure calculations suggest that the dominating bands for the electron conduction are originated from the Bi 6p orbitals in the BiS_2 layer [11, 12]. A recent study has found that there are two distinct phases related to $Bi_4O_4S_3$, which are namely $Bi_3O_2S_3$ and Bi_2OS_2. The $Bi_3O_2S_3$ phase is responsible for the change of superconducting volume fraction [13]. The nominal composition $Bi_4O_4S_3$ is widely used, but the actual composition remains controversial.

Doping has always been regarded as an effective way in the exploring of new superconducting materials and the investigating of the physical properties of a superconductor. To compare the substitution effects in Bi site by metals of different valence, we systematically investigate the doping effects of isovalent Sm and bivalent Pb on the physical properties and superconductivity of $Bi_4O_4S_3$. Resistivity, magnetization, and Hall effect measurements are performed to investigate the difference in the effects of Pb doping and Sm doping. We make a detailed discussion on the reason of the difference, which can provide some clues about how superconductivity is destroyed. We believe the present results are helpful in better understanding of the superconducting properties of $Bi_4O_4S_3$.

X. Yao · J. Shao · Z. Liu · L. Zhang · C. Zhang (✉) · Y. Zhang
High Magnetic Field Laboratory, Chinese Academy of Sciences and University of Science and Technology of China, Hefei 230026, People's Republic of China
e-mail: zhangcj@hmfl.ac.cn

X. Yao · J. Shao · Z. Liu · S. Tan · C. Zhang · Y. Zhang
Hefei National Laboratory for Physical Sciences at the Microscale, University of Science and Technology of China, Hefei 230026, People's Republic of China

2 Experiment

The polycrystalline samples of $Bi_{4-x}Sm_xO_4S_3$ ($0 \leq x \leq 0.16$) and $Bi_{4-x}Pb_xO_4S_3$ ($0 \leq x \leq 0.1$) were synthesized through a conventional solid-state reaction method. Starting materials of Bi_2S_3 (99.999 %, Alfa Aesar), Sm (99.9 %, Alfa Aesar), Pb (99.9 %, Alfa Aesar), Bi_2O_3 (99.9 %, Alfa Aesar), and S (99.5 %, Alfa Aesar) were weighed in stoichiometric ratio, fully ground, and then pressed into pellets. The pellets were sealed into an evacuated (2×10^{-5} Torr) quartz tube and heated at 510 ° for 12 h. The obtained pellets were ground again and the above treatment was repeated. The obtained samples were characterized by powder X-ray diffraction with Cu K_α radiation at room temperature. Resistivity and Hall effect measurements within 2–300 K were taken using a four-probe method on a Quantum Design Physical Property Measurement System (PPMS). The Hall effect measurement was performed by sweeping the magnetic field up to 9 T at fixed temperature. Magnetic properties were measured using a superconducting quantum interference device (SQUID) magnetometer.

3 Results and Discussion

Figure 1a gives the powder X-ray diffraction (XRD) patterns of the $Bi_{4-x}Sm_xO_4S_3$ ($0 \leq x \leq 0.12$) and $Bi_{4-x}Pb_xO_4S_3$ ($0 \leq x \leq 0.1$) samples. The Bragg diffraction peaks are indexed with the tetragonal structure (space group: I4/mmm). From the XRD results, we find that the $Bi_4O_4S_3$ sample exhibiting better quality than previous reports [3, 4]. The calculated lattice parameters of $Bi_4O_4S_3$ are $a = 3.9545(2)$ Å and $c = 41.1258(3)$ Å. In order to clearly see the variation of the lattice parameters with the Sm and Pb doping, we plot an enlarged view of both the (006) and (110) diffraction peaks. The results are shown in Fig. 1b, c. It is found that both the (006) and (110) peaks shift towards lower angles with increasing Sm or Pb doping, indicating the increase of the lattice constants with Sm and Pb doping. For example, the calculated lattice parameters of $Bi_{3.92}Sm_{0.08}O_4S_3$ are $a = 3.9606(4)$ Å and $c = 41.3081(2)$ Å. And, the lattice constants of $Bi_{3.92}Pb_{0.08}O_4S_3$ are $a = 3.9665(1)$ Å and $c = 41.3411(2)$ Å. The change of lattice parameters confirms that Sm and Pb are substantially incorporated into the $Bi_4O_4S_3$ lattice. A minority of Bi_2S_3 impurities appears with increasing doping concentration, which is common in the solid-state reaction process under ambient pressure [3, 4].

Figure 2a, b gives the temperature dependence of the dc magnetic susceptibility measured at $H = 20$ Oe for the $Bi_{4-x}Sm_xO_4S_3$ ($0 \leq x \leq 0.16$) and $Bi_{4-x}Pb_xO_4S_3$ ($0 \leq x \leq 0.1$) samples. Diamagnetic signal appears below 4.6 K in the undoped $Bi_4O_4S_3$ sample, confirming the occurrence of superconductivity. With increasing doping concentration, the superconducting transition temperature (T_c) gradually decreases in both the Sm-doped samples and the Pb-doped samples. For example, the T_c value for $Bi_{3.88}Sm_{0.12}O_4S_3$ sample is about 3.6 K and it is about 3.8 K for $Bi_{3.92}Pb_{0.08}O_4S_3$ sample. Simultaneously, the shielding volume fraction reduces with increasing doping content in both the Sm-doped samples and the Pb-doped samples. It is found that the diamagnetic signal vanishes at a relatively lower doping content in Pb-doped samples compared with that in the Sm-doped samples. For example, the $Bi_{3.9}Pb_{0.1}O_4S_3$ sample hardly exhibits any diamagnetic signal above 2 K, while in $Bi_{3.88}Sm_{0.12}O_4S_3$ sample, apparent diamagnetic signal appears below 3.6 K. These facts suggest that the bivalent Pb doping leads to more severe depression on the superconductivity of $Bi_4O_4S_3$ compared with the isovalent Sm doping.

It is worth noticing that the Pb doping leads to severe depression of superconductivity in $Bi_4O_4S_3$ system, which is in sharp contrast to the enhancement of superconductivity in Pb-substituted Bi-Sr-Ca-Cu-O system. Partial

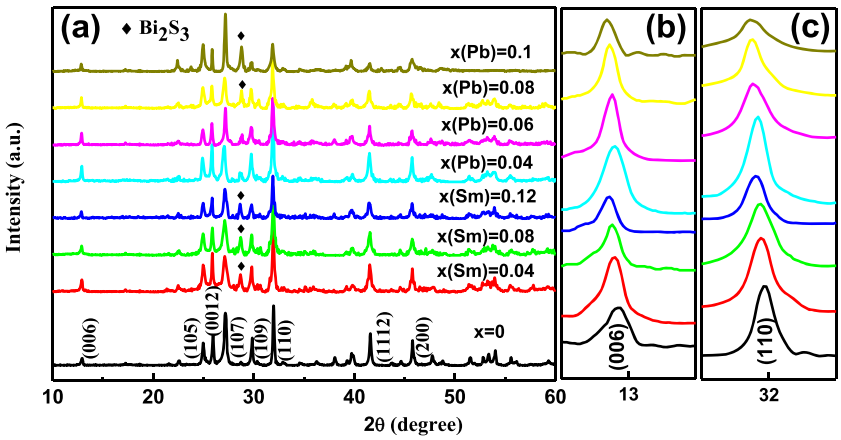

Fig. 1 (*Color online*) **a** Powder X-ray diffraction patterns for $Bi_{4-x}Sm_xO_4S_3$ ($0 \leq x \leq 0.12$) and $Bi_{4-x}Pb_xO_4S_3$ ($0 \leq x \leq 0.1$). Miller indices are displayed for the undoped $Bi_4O_4S_3$ sample **b** The enlarged details around the (006) peak for all samples **c** The enlarged details around the (110) peak for all samples

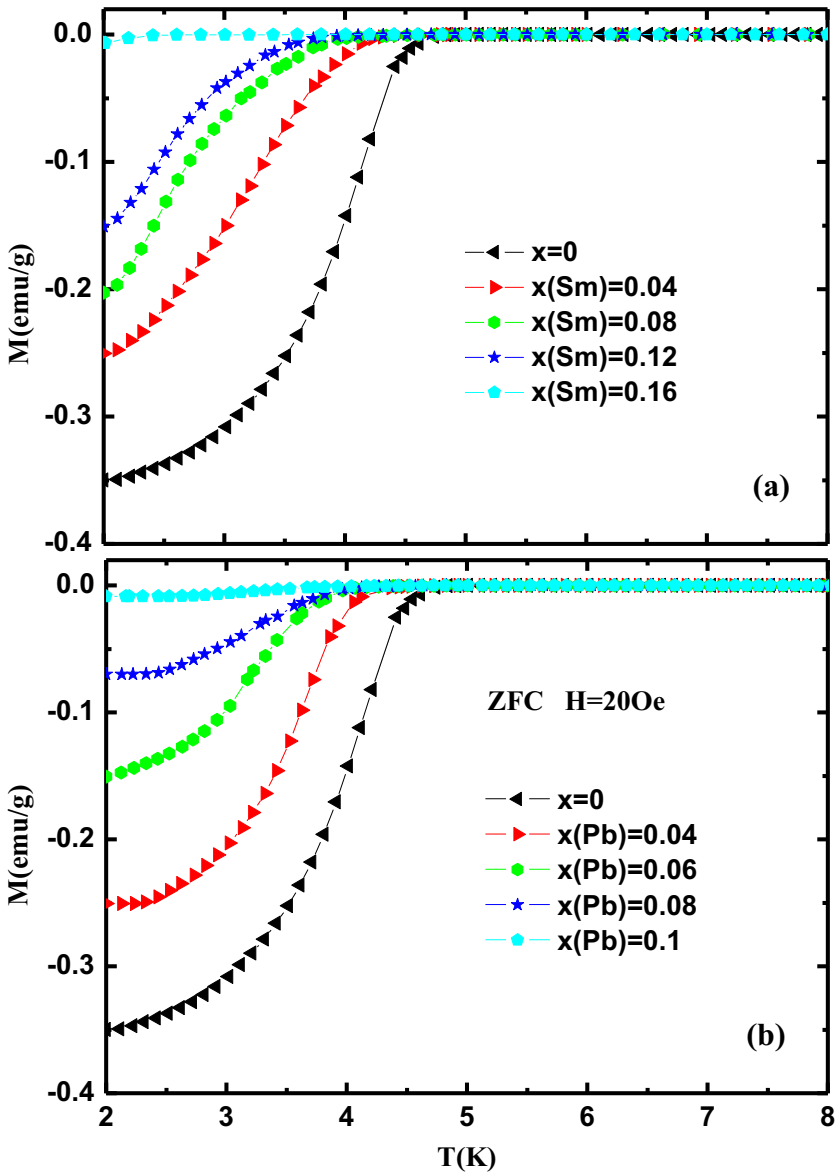

Fig. 2 (*Color online*) Temperature dependence of the magnetic susceptibility under applied magnetic field of 20 Oe for **a** $Bi_{4-x}Sm_xO_4S_3$ ($x = 0$, 0.04, 0.08, 0.12 and 0.16) and **b** $Bi_{4-x}Pb_xO_4S_3$ ($x = 0$, 0.04, 0.06, 0.08 and 0.1) samples. The measurements are performed under zerofield cooling process

substitution of Pb for Bi in the Bi-Sr-Ca-Cu-O system has been found to be highly advantageous to the formation of the high-T_c phase and improve the critical current density J_c [14, 15]. The discordance in these two systems is probably due to the different role of Bi in the structure of $Bi_4O_4S_3$ and Bi-Sr-Ca-Cu-O system. In Bi-Sr-Ca-Cu-O system, only BiO spacer layers contain Bi atoms, while in $Bi_4O_4S_3$, both Bi_2O_2 spacer layers and BiS_2 superconducting layers contain Bi atoms. Another possible reason is related to the different types of charge carriers between $Bi_4O_4S_3$ superconductor and Bi-Sr-Ca-Cu-O superconductor. In $Bi_4O_4S_3$, electron-type charge carriers dominate the conductivity. On the contrary, the conductivity is dominated by hole-type carriers in the Bi-Sr-Ca-Cu-O system. The substitution of bivalent Pb for trivalent Bi introduces hole-type carriers, which leads to the decrease of electron-type charge carriers in $Bi_4O_4S_3$ system. In contrast, the substitution of Pb for Bi in the Bi-Sr-Ca-Cu-O system results in an increase of hole-type charge carrier concentration, which is favorable for the superconductivity in the Bi-Sr-Ca-Cu-O system.

Figure 3a, b shows the temperature dependence of the resistivity for $Bi_{4-x}Sm_xO_4S_3$ ($0 \leq x \leq 0.12$) and $Bi_{4-x}Pb_xO_4S_3$ ($0 \leq x \leq 0.1$) samples, respectively. The insets show the temperaturedependent resistivity over the extended temperature range of 2–300 K. Resistivity of all the samples except $Bi_{3.9}Pb_{0.1}O_4S_3$ shows linear temperature dependence between 50 and 300 K, indicative of a metallic-like behavior. It is found that the normal-state resistivity of both the Sm-doped samples and Pb-doped samples increases with increasing doping concentration, suggesting the decrease of effective charge carriers. The T_c^{onset} and T_c^{zero} of undoped sample $Bi_4O_4S_3$ are 5.0 and 4.3 K,

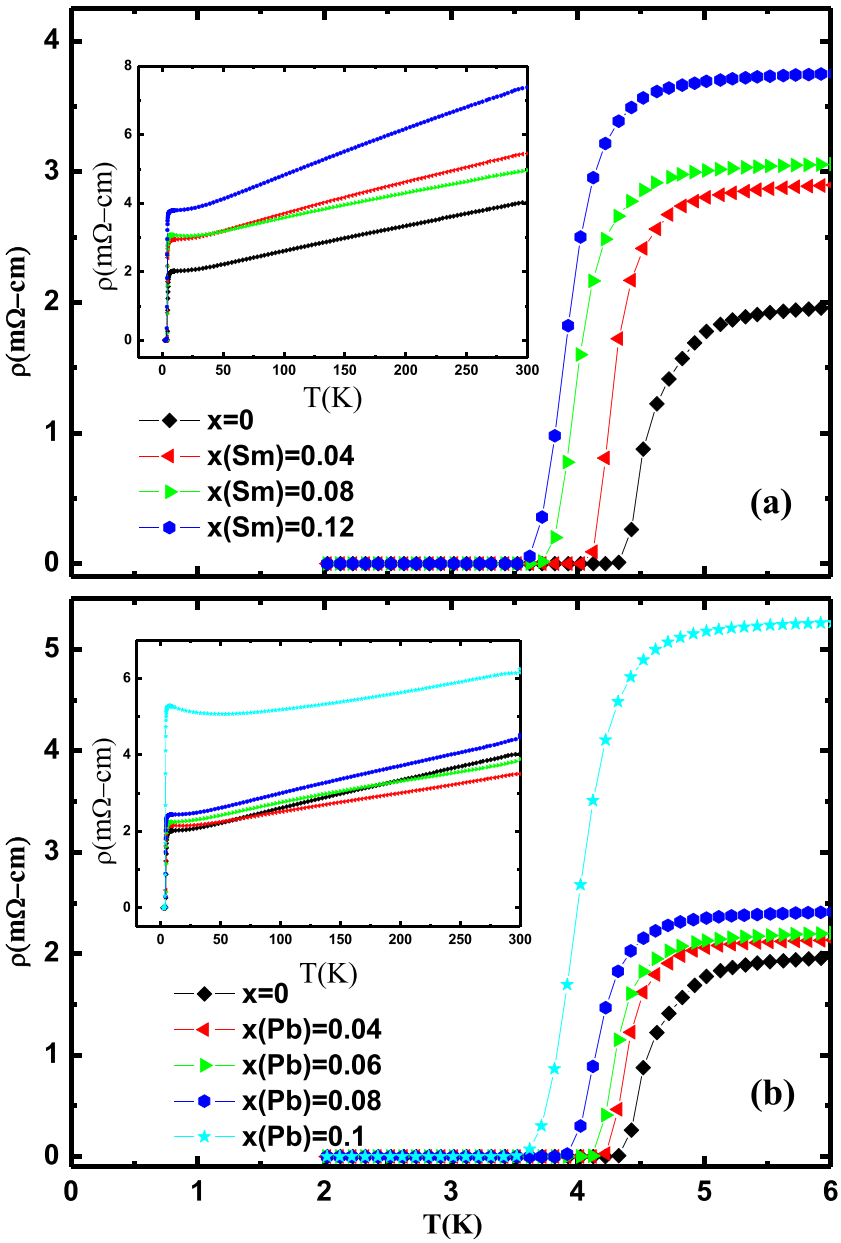

Fig. 3 (*Color online*) Temperature dependence of the resistivity under zero magnetic field for **a** $Bi_{4-x}Sm_xO_4S_3$ ($x = 0$, 0.04, 0.08 and 0.12) and **b** $Bi_{4-x}Pb_xO_4S_3$ ($x = 0$, 0.04, 0.06, 0.08 and 0.1) samples in the temperature range 2–6 K. *Inset* of the figure shows the same over the extended temperature range of 2–300 K

respectively. From Fig. 3, we find that the superconducting transition temperature shifts to lower temperature with increasing Sm doping concentration, which is in agreement with the result from magnetic susceptibility. From the resistivity data, it is also found that the bivalent Pb doping suppresses the superconductivity of $Bi_4O_4S_3$ more severely compared with the isovalent Sm doping. For example, the T_c^{zero} drops to 3.6 K at the doping concentration of $x = 0.12$ in Sm-doped sample, while the T_c^{zero} drops to 3.5 K at a lower doping concentration of $x = 0.1$ in Pb-doped sample.

The temperature dependence of resistivity under magnetic field up to 6 T of the $Bi_4O_4S_3$, $Bi_{3.92}Sm_{0.08}O_4S_3$, and $Bi_{3.92}Pb_{0.08}O_4S_3$ samples is shown in Fig. 4a–c, respectively. Compared with the undoped $Bi_4O_4S_3$ sample, the superconductivity of Sm-doped samples and Pb-doped samples is more fragile under applied magnetic field. Under a magnetic field of 0.5 T, zero resistivity cannot be observed even down to the lowest temperature of 2 K for $Bi_{3.92}Sm_{0.08}O_4S_3$ and $Bi_{3.92}Pb_{0.08}O_4S_3$ samples, while for $Bi_4O_4S_3$, one can clearly see the zero resistivity at above 2 K. The broadening of the superconducting transition under applied magnetic field implies the strong superconducting fluctuation in $Bi_4O_4S_3$, in agreement with the scanning tunneling spectroscopy measurements [16]. A moderate magnetoresistance is observed in all samples, which is believed to be caused by multi-band effect. For $Bi_{3.92}Sm_{0.08}O_4S_3$,

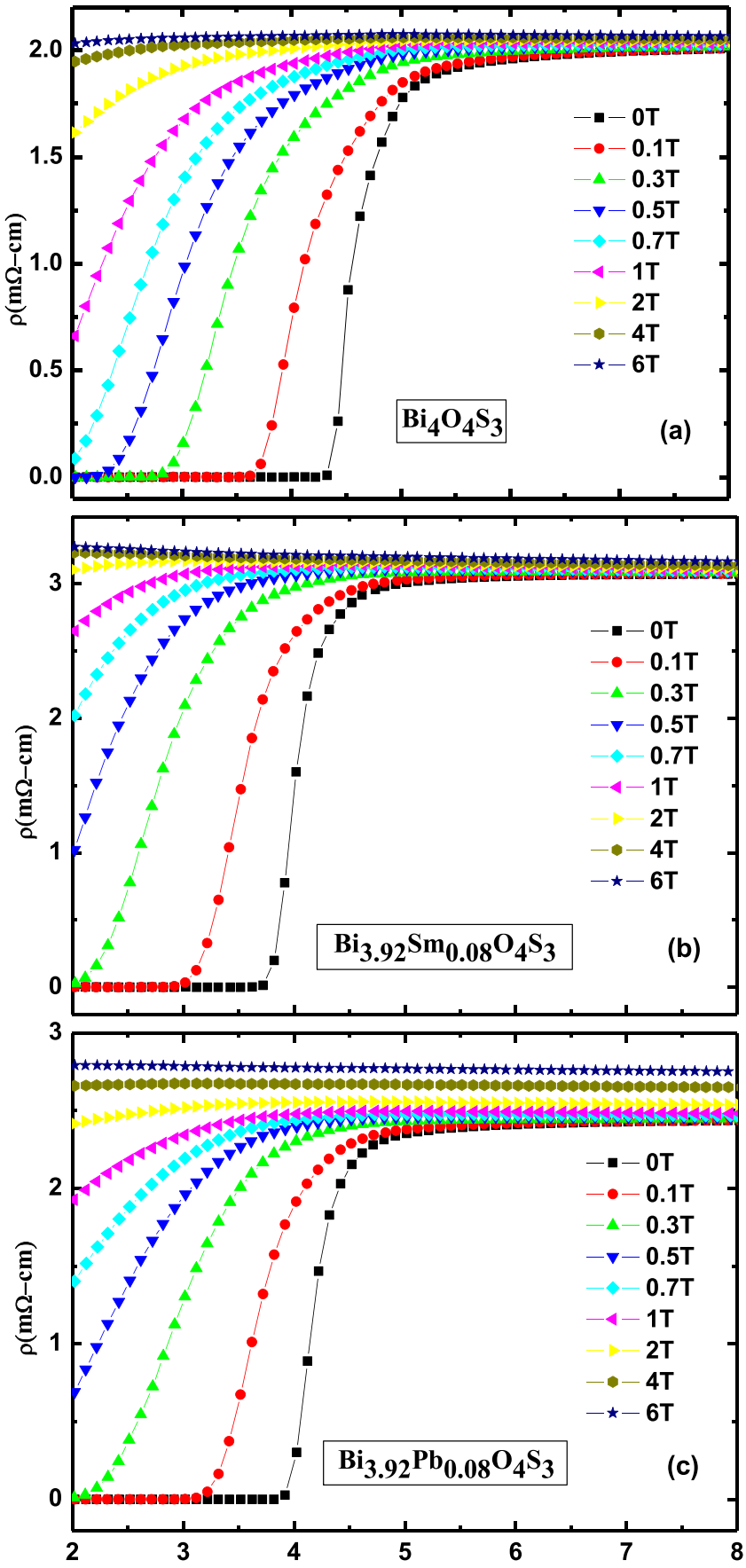

Fig. 4 (*Color online*) Temperature dependence of the resistivity under magnetic fields of 0, 0.1, 0.3, 0.5, 0.7, 1, 2, 4, and 6 T for **a** $Bi_4O_4S_3$, **b** $Bi_{3.92}Sm_{0.08}O_4S_3$, and **c** $Bi_{3.92}Pb_{0.08}O_4S_3$, respectively

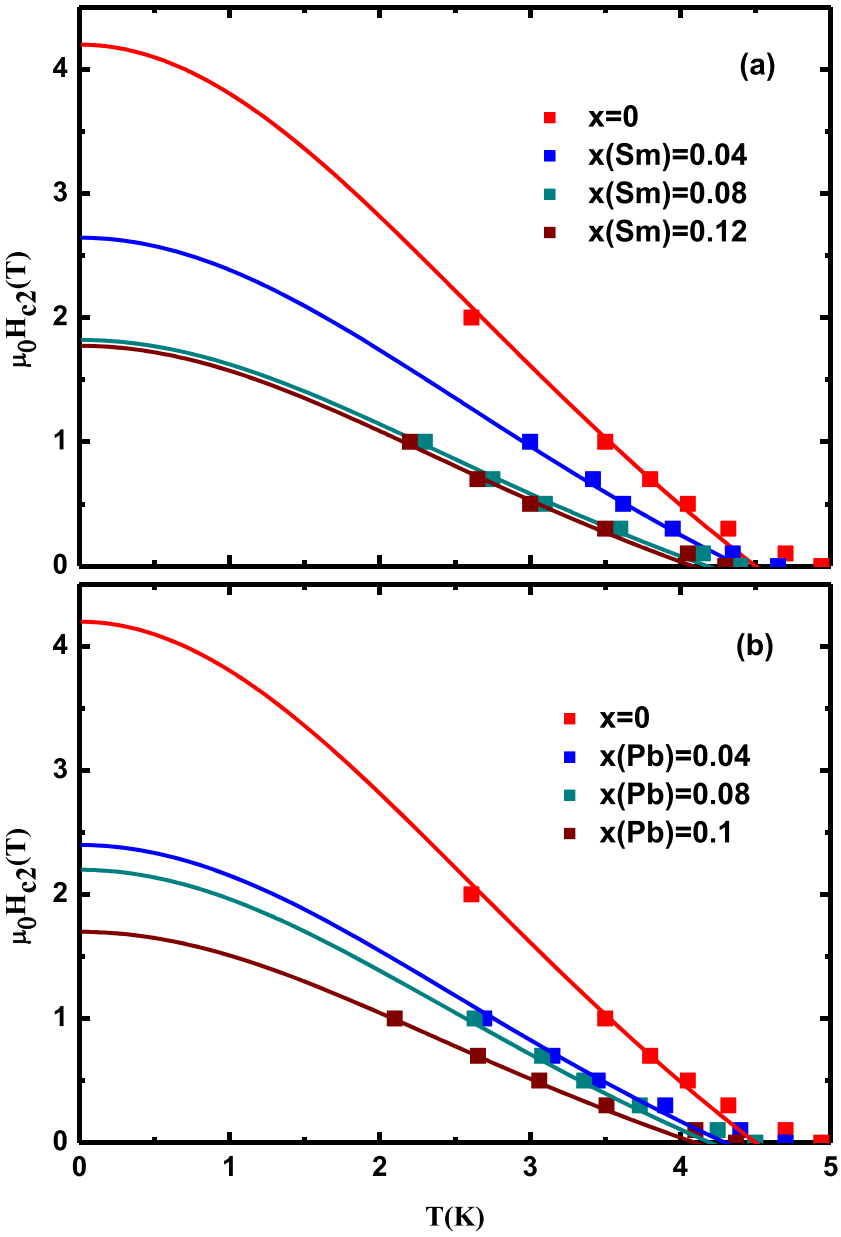

Fig. 5 (*Color online*) The upper critical field $H_{c2}(T)$ obtained from 90 % normal-state resistivity criterion for **a** $Bi_{4-x}Sm_xO_4S_3$ ($x = 0$, 0.04, 0.08 and 0.12) and **b** $Bi_{4-x}Pb_xO_4S_3$ ($x = 0$, 0.04, 0.08 and 0.1) respectively. The *solid lines* are the fitting data using $H_{c2}(T) = H_{c2}(0)(1 - t^2)/(1 + t^2)$

a weak insulating behavior is induced by applied magnetic field. The insulating behavior could be induced by the polarized electrons caused by the Zeeman effect [17].

The upper critical field, $H_{c2}(T)$, is determined by using the 90 % normal-state resistivity criterion. The obtained $H_{c2}(T)$ values for $Bi_{4-x}Sm_xO_4S_3$ ($0 \leq x \leq 0.12$) and $Bi_{4-x}Pb_xO_4S_3$ ($0 \leq x \leq 0.1$) are given in Fig. 5a, b, respectively. The $H_{c2}(0)$ value is estimated by fitting the $H_{c2}(T)$ data using $H_{c2}(T) = H_{c2}(0)(1-t^2)/(1+t^2)$, where $t = T/T_c$ is the reduced temperature and $H_{c2}(0)$ is the upper critical field at zero temperature. The solid lines are the fitting data. The obtained $H_{c2}(0)$ value of $Bi_4O_4S_3$ is 4.2 T, while the $H_{c2}(0)$ value drops to 1.8 T in $Bi_{3.88}Sm_{0.12}O_4S_3$ and 1.7 T in $Bi_{3.9}Pb_{0.1}O_4S_3$. The present results suggest that the $H_{c2}(T)$ value is suppressed in both Sm-doped samples and Pb-doped samples. The bivalent Pb doping leads to more rapid decrease of $H_{c2}(T)$ compared with Sm doping.

In order to investigate the change-on-charge carrier concentration, we perform the measurements of Hall effect on the $Bi_4O_4S_3$, $Bi_{3.88}Sm_{0.12}O_4S_3$, and $Bi_{3.9}Pb_{0.1}O_4S_3$ samples. Figure 6a shows the magnetic field dependence of the transverse resistivity (ρ_{xy}) at different temperatures for $Bi_4O_4S_3$. It is found that the ρ_{xy} value is negative at all temperature, suggesting that electron is the dominating carrier in this compound. We use a simple approximation $R_H = \rho_{xy}/H$ to calculate the Hall coefficient R_H from the transverse resistivity data. In Fig. 6b, the Hall

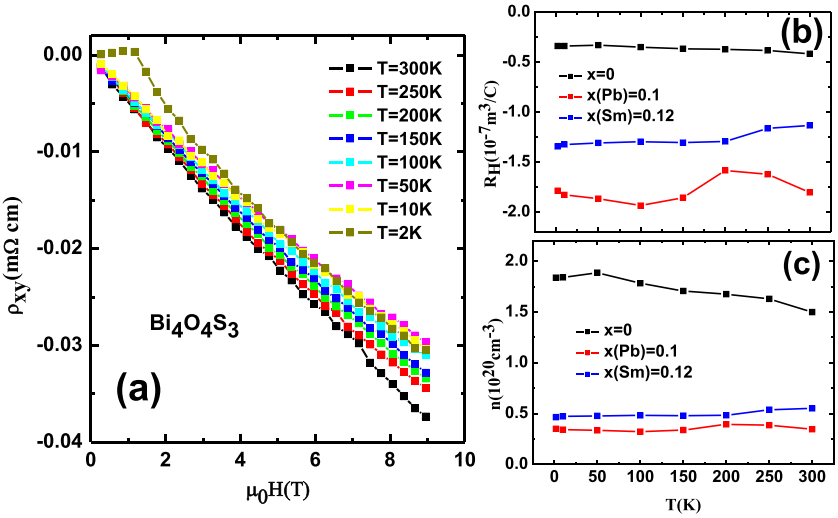

Fig. 6 (*Color online*) **a** The transverse resistivity ρ_{xy} versus the magnetic field μH at different temperatures for sample $Bi_4O_4S_3$. **b** The Hall coefficient R_H calculated at 9 T for $Bi_4O_4S_3$, $Bi_{3.9}Pb_{0.1}O_4S_3$, and $Bi_{3.88}Sm_{0.12}O_4S_3$ as a function of temperature. **c** The carrier concentration deduced from Hall coefficient for $Bi_4O_4S_3$, $Bi_{3.9}Pb_{0.1}O_4S_3$, and $Bi_{3.88}Sm_{0.12}O_4S_3$ as a function of temperature

coefficient R_H is plotted as the function of temperature for $Bi_4O_4S_3$, $Bi_{3.88}Sm_{0.12}O_4S_3$, and $Bi_{3.9}Pb_{0.1}O_4S_3$. It is found that the Hall coefficient slightly changes with the variation of temperature for all samples. Both the Sm and Pb doping at the Bi site do not change the sign of R_H, but the absolute value of R_H increases for about three to four times in $Bi_{3.88}Sm_{0.12}O_4S_3$ and $Bi_{3.9}Pb_{0.1}O_4S_3$ comparing to that in $Bi_4O_4S_3$ sample. The change of R_H reflects the decreasing of carrier concentration in Sm-doped samples and Pb-doped samples. The estimated charge carrier density at different temperatures is given in Fig. 6c. The carrier density of $Bi_4O_4S_3$ is about 1.5×10^{20} cm^{-3} at 300 K, while the carrier density is decreased to about 3.5×10^{19} cm^{-3} in $Bi_{3.9}Pb_{0.1}O_4S_3$ and about 5.5×10^{19} cm^{-3} in $Bi_{3.88}Sm_{0.12}O_4S_3$.

The much faster decrease in charge carrier density in Pb-doped samples comparing to that in Sm-doped samples could be due to the difference in the valence states. As revealed by Hall coefficient measurements, the dominating carrier in $Bi_4O_4S_3$ is electron-type. The partial substitution of bivalent Pb at the trivalent Bi site introduces hole-type charge carriers, resulting in the sharp decrease in electron-type charge carrier concentration. It should also be noticed that the isovalent Sm doping leads to the decrease of charge carrier concentration. Previous band structure calculation suggests that the dominating bands for electron conduction originated from the Bi 6p orbitals in the BiS_2 layer [11, 12]. For Sm ion, the 6p orbitals are empty; thus, the Sm 6p orbitals do not involve in the electron conduction in the Sm-doped samples. In this sense, the Sm dopants can be regarded as impurity scatterers, which block the conduction in the Sm-doped samples. Due to these facts, the effects of Sm doping in the $Bi_4O_4S_3$ system are due to the localization of charge carriers. On the other hand, the substitution of Bi by Pb introduces hole-type charge carriers, which leads to the significant decrease of electron-type charge carriers. Thus, the suppression of superconductivity is more severe in the Pb-doped samples compared with the Sm-doped samples.

4 Conclusion

In summary, the effects of bivalent Pb doping and trivalent Sm doping on the superconductivity of $Bi_4O_4S_3$ superconductor have been investigated by a systematical study on the transport and magnetic properties of $Bi_{4-x}Sm_xO_4S_3$ ($0 \le x \le 0.16$) and $Bi_{4-x}Pb_xO_4S_3$ ($0 \le x \le 0.1$) samples. It is found that the bivalent Pb doping leads to more severe depression on the superconductivity comparing to the isovalent Sm doping. We notice that the Sm 6p orbitals make no contribution to the electron conduction, which means that Sm dopants act as the impurity scatterers. The substitution of Bi by Pb introduces hole-type charge carriers, which gives rise to the significant decrease of electron-type charge carriers. The more severe suppression effect of bivalent Pb doping compared with Sm doping might be helpful in better understanding of the superconducting properties of $Bi_4O_4S_3$.

Acknowledgments This work was supported by the State Key Project of Fundamental Research of China (Grant Nos. 2010CB923403 and 2011CBA00111) and the Natural Science Foundation of China (Grant Nos. 11174290 and U1232142).

References

1. Kamihara, Y., Watanabe, T., Hirano, M., Hosono, H.: J. Am. Chem. Soc. **130**, 3296 (2008)
2. Chen, X.H., Wu, T., Wu, G., Liu, R.H., Chen, H., Fang, D.F.: Nat. (London) **453**, 761 (2008)

3. Singh, S.K., Kumar, A., Gahtori, B., Sharma, G., Patnaik, S., Awana, V.P.S.: J. Am. Chem. Soc. **134**, 16504 (2012)
4. Mizuguchi, Y., Fujihisa, H., Gotoh, Y., Suzuki, K., Usui, H., Kuroki, K., Demura, S., Takano, Y., Izawa, H., Miura, O.: Phys. Rev. B **86**, 220510(R) (2012)
5. Mizuguchi, Y., Demura, S., Deguchi, K., Takano, Y., Fujihisa, H., Gotoh, Y., Izawa, H., Miura, O.: J. Phys. Soc. Jpn. **81**, 114725 (2012)
6. Jha, R., Kumar, A., Singh, S.K., Awana, V.P.S.: J. Supercond. Nov. Magn. **26**, 499 (2013)
7. Jha, R., Kumar, A., Singh, S.K., Awana, V.P.S.: J. Appl. Phys. **113**, 056102 (2013)
8. Xing, J., Li, S., Ding, X.X., Yang, H., Wen, H.H.: Phys. Rev. B **86**, 214518 (2012)
9. Lin, X., Ni, X.X., Chen, B., Xu, X.F., Yang, X.X., Dai, J.H., Li, Y.K., Yang, X.J., Luo, Y.K., Tao, Q., Cao, G.H., Xu, Z.: Phys. Rev. B **87**, 020504(R) (2013)
10. Jha, R., Tiwari, B., Awana, V.P.S.: J. Phys. Soc. Jpn. **83**, 063707 (2014)
11. Usui, H., Suzuki, K., Kuroki, K.: Phys. Rev. B **86**, 220501(R) (2012)
12. Mizuguchi, Y., Fujihisa, H., Gotoh, Y., Suzuki, K., Usui, H., Kuroki, K., Demura, S., Takano, Y., Izawa, H., Miura, O.: Phys. Rev. B **86**, 220510(R) (2012)
13. Phelan, W.A., Wallace, D.C., Arpino, K.E., Neilson, J.R., Livi, K.J., Seabourne, C.R., Scott, A.J., McQueen, T.M.: J. Am. Chem. Soc. **135**, 5372 (2013)
14. Togano, K., Kumakura, H., Maeda, H., Yanagisawa, E., Takahashi, K.: Appl. Phys. Lett. **53**, 1329 (1988)
15. Takano, M., Takada, J., Oda, K., Kitaguchi, H., Miura, Y., Ikeda, Y., Tomii, Y., Mazaki, H.: Jpn. J. Appl. Phys. **27**, L1041
16. Li, S., Yang, H., Tao, J., Ding, X.X., Wen, H.H.: Sci. China-Phys. Mech. Astron. **56**, 2019 (2013)
17. Li, S., Yang, H., Tao, J., Ding, X.X., Wen, H.H.: arXiv:1207.4955